Original Article

Post-operative pediatric cerebellar mutism syndrome and its association with hypertrophic olivary degeneration

Shivaram Avula[1], Michaela Spiteri[2], Ram Kumar[3], Emma Lewis[2], Srikrishna Harave[1], David Windridge[2], Chan Ong[1], Barry Pizer[4]

[1]Department of Radiology, Alder Hey Children's NHS Foundation, Liverpool, UK; [2]Centre for Vision, Speech and Signal Processing, University of Surrey, Guildford, UK; [3]Department of Neurology, [4]Department of Oncology, Alder Hey Children's NHS Foundation, Liverpool, UK

Correspondence to: Dr. Shivaram Avula. Department of Radiology, Alder Hey Children's NHS Foundation Trust, Eaton Road, West Derby, Liverpool L12 2AP, UK. Email: shivaram.avula@alderhey.nhs.uk.

Background: The dentato-thalamo-cortical (DTC) pathway is recognized as the anatomical substrate for postoperative pediatric cerebellar mutism (POPCMS), a well-recognized complication affecting up to 31% of children undergoing posterior fossa brain tumour resection. The proximal structures of the DTC pathway also form a segment of the Guillain and Mollaret triangle, a neural network which when disrupted causes hypertrophic olivary degeneration (HOD) of the inferior olivary nucleus (ION). We hypothesize that there is an association between the occurrence of POPCMS and HOD and aim to evaluate this on MR imaging using qualitative and quantitative analysis of the ION in children with and without POPCMS.

Methods: In this retrospective study we qualitatively analysed the follow up MR imaging in 48 children who underwent posterior fossa tumour resection for presence of HOD. Quantitative analysis of the ION was possible in 28 children and was performed using semi-automated segmentation followed by feature extraction and feature selection techniques and relevance of the features to POPCMS were evaluated. The diagnosis of POPCMS was made independently based on clinical and nursing assessment notes.

Results: There was significant association between POPCMS and bilateral HOD (P=0.002) but not unilateral HOD. Quantitative analysis showed that hyperintensity in the left ION was the most relevant feature in children with POPCMS.

Conclusions: Bilateral HOD can serve as a reliable radiological indicator in establishing the diagnosis of POPCMS particularly in equivocal cases. The strong association of signal change due to HOD in the left ION suggests that injury to the right proximal efferent cerebellar pathway plays an important role in the causation of POPCMS.

Keywords: Cerebellar mutism syndrome (CMS); hypertrophic olivary degeneration; posterior fossa syndrome (PFS); postoperative pediatric cerebellar mutism syndrome

Submitted Sep 17, 2016. Accepted for publication Oct 10, 2016.
doi: 10.21037/qims.2016.10.11
View this article at: http://dx.doi.org/10.21037/qims.2016.10.11

Introduction

Post-operative cerebellar mutism is a well-recognized complication that affects children undergoing posterior fossa brain tumour resection. It has been known by various names including posterior fossa syndrome (PFS) and cerebellar mutism syndrome (CMS). For the purpose of uniformity, we choose to use 'postoperative pediatric cerebellar mutism syndrome' (POPCMS), the term coined following a recent consensus among an international working group of clinicians and scientists to avoid confusion with other disorders with similar clinical features among children and adults (1). The incidence of this disorder varies between 8% and 31% (2) following posterior fossa tumour resection. It is characterized by delayed onset mutism and

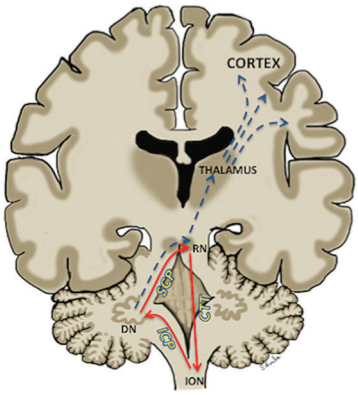

Figure 1 Diagram showing the dentato-thalamo-cortical pathway (blue) and the Guillain and Mollaret triangle (red). DN, dentate nucleus; RN, red nucleus; ION, inferior olivary nucleus; SCP, superior cerebellar peduncle; CTT, central tegmental tract; ICP, inferior cerebellar pathway.

emotional lability but other symptoms such as hypotonia and oropharyngeal dysfunction may also accompany the condition (1). Mutism is always transient but is often followed by varying periods of dysarthria and long-term neurological deficits including ataxia and cognitive disorders (1,3,4).

There is growing consensus on the anatomical substrates involved in the causation of POPCMS and interruption of the dentato-thalamo-cortical (DTC) pathway has been attributed to its aetiology (*Figure 1*) (5-7). The proximal efferent cerebellar pathway (pECP), which forms the proximal segment of the DTC, has been attributed as the region of primary post surgical insult (8-14). The pECP mainly constitutes the dentate nucleus (DN), the superior cerebellar peduncle (SCP) and the mesencephalic tegmentum (MT). These structures are often situated close to the tumour and are prone to damage during surgical resection. Bilateral injury of the pECP has been associated with a greater risk of development of POPCMS (8,10,12,15). Although surgical injury has been attributed to POPCMS, the exact underlying pathophysiology remains unclear and various hypotheses have been proposed (16).

The SCP, which carries efferent cerebellar fibers of the pECP from DN to the contralateral red nucleus, also forms a component of the dentato-rubro-olivary pathway known as "Guillain-Mollaret triangle". This triangular network is formed by the red nucleus, the ipsilateral inferior olivary nucleus (ION) and the contralateral DN. The red nucleus is connected to the ipsilateral ION by the central tegmental tract and receives afferents from the contralateral DN through the SCP. The triangle is completed by efferent fibers connecting the ION to the contralateral DN through the inferior cerebellar peduncle (*Figure 1*). Disruption of the triangle results in hypertrophic degeneration of the ION, which is thought to represent retrograde trans-synaptic degeneration of the ION. Injury to the DN and SCP leads to contralateral hypertrophic olivary degeneration (HOD) and injury to the red nucleus and central tegmental tract results in ipsilateral HOD. HOD can be identified on MRI scan as hypertrophy and/or hyperintensity of the ION on the T2 weighted images (17).

As the DTC pathway and the Guillain-Mollaret triangle contain common structures, we hypothesized that there was a relationship between the occurrence of HOD and POPCMS. In this study we aimed to evaluate the changes related to the inferior olivary nuclei in children who underwent posterior fossa tumour resection. We performed independent qualitative and quantitative analyses of the ION. The results of the quantitative analysis has been published earlier focusing on the technical aspect of the analysis (18). In this article we aim to combine the results of the analyses and discuss their clinical relevance.

Methods

This was a retrospective study evaluating the MRI scans of children who underwent posterior fossa tumor resection at our institution between July 2007 and December 2012. Forty-eight children underwent the surgery during this period. Twenty-eight of them were girls and the mean age was 8.1 years. Of the 48 children, the pathological diagnoses were pilocytic astrocytoma in 22, ependymoma in 12, medulloblastoma in 7, atypical teratoid rhabdoid tumour in 2, oligodendroglioma in 2 and one case each of grade II astrocytoma, neurilemmoma and haemangioma. The clinical and nursing notes of these children were independently reviewed by an experienced paediatric neurologist for evidence of POPCMS. Since there was no agreed defenitions for POPCMS at the time of the study, the diagnostic criteria was based on existing literature and clinical experience (8). The diagnostic criteria for POPCMS was delayed onset mutism or marked reduction in speech output with or without irritability or lack of volitional movement persisting for more than 7 days following surgery. Children whose symptoms could be explained by other mechanisms such as infection and hydrocephalus were not regarded to have POPCMS. The study methodology

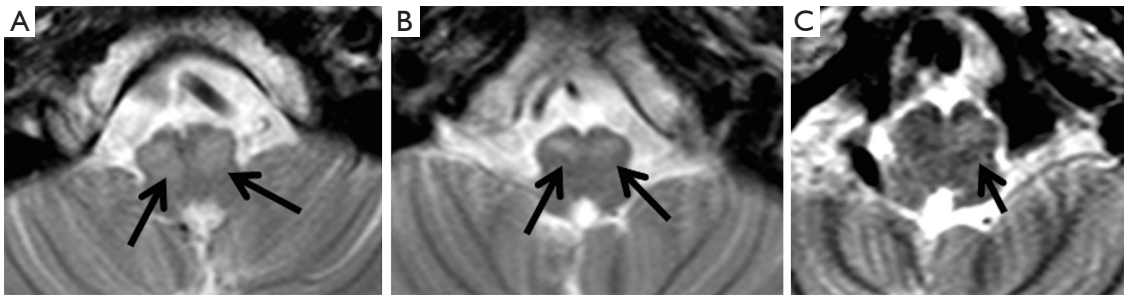

Figure 2 Axial T2 weighted images of the posterior fossa at the level of the inferior olivary nuclei demonstrating bilateral hypertrophy and hyperintensity of the ION (A), bilateral hyperintensity of the ION (B) and unilateral hyperintensity of the left ION (C). ION, inferior olivary nucleus.

was granted approval by the Institutional Research Director.

MR Imaging

The MRI scans were performed on 1.5 T Philips Achieva (Best, Netherlands) and 3 T XL Philips Achieva (Best, Netherlands) MR scanners. The preoperative, immediate postoperative scans and all follow up scans until 12 months post surgery were anonymised for evaluation. Since November 2009 patients underwent surgical resection with the aid of intraoperative MRI (ioMRI) where an MR scan was performed to check for completeness of tumour resection prior to surgical closure. The ioMRI scanner was located in a room adjacent to the operating theatre and the patient was transported to and from the scanner during the course of the surgery. Usually one, two or occasionally three ioMRI scans were performed until the surgical aim was achieved (19,20). In these patients, the final intraoperative MRI scan was regarded as the immediate postoperative baseline scan. For the purpose of this study, the ION was assessed for evidence of HOD on the axial T2 turbo spin echo sequence. The MRI parameters on the 3 T magnet was TR =3,000 ms, TE =80 ms, Echo train length =15, matrix 400×319, field of view =230 mm, slice thickness =4 mm and slice gap =1 mm. The parameters on the 1.5 T magnet was TR =4,924 ms, TE =110 ms, echo train length =15, matrix 384×306, field of view =230 mm, slice thickness =5 mm and slice spacing =1 mm. Excluding the immediate post-operative scan, the number of follow up scans during the first year post surgery varied between 1 and 4 with the average number of scans being 3.

Qualitative analysis of the imaging

Two consultant radiologists with 8 and 6 years' experience in paediatric neuroradiology reviewed the anonymised axial T2 weighted scans independently. They were blinded from the clinical information and the diagnosis of POPCMS. The IONs were assessed for the evidence of unilateral or bilateral HOD. Unequivocal T2 prolongation (hyperintensity) with/without unequivocal hypertrophy of the ION was considered to be positive for HOD. Unequivocal T2 prolongation of the center/hilum of the ION was also regarded as positive for HOD (*Figure 2*). Cases where T2 prolongation in the ION was equivocal were not considered to have HOD. Pre-operative MRI scan images were reviewed to ensure the absence of HOD prior to surgery. Discrepancies between both observers were resolved through consensus.

Quantitative analysis

The quantitative analysis of the MR imaging was performed in collaboration with The Centre for Vision, Speech and Signal Processing at the University of Surrey, UK. A detailed account of the analysis methodology and outcome has been published in an earlier article (18). In order to analyze the changes in the left and right ION with respect to their original state pre-operatively it was required to assess their state in the pre-operative scan, as well as on at least two post-operative scans. This resulted in three data points over which the average gradient could be computed.

Some subjects whose pre-operative scan was not included in the dataset had to be eliminated from this part of the study. If tumorous tissue or scar tissue occluded the ION in an MR image then it was not possible to delineate each ION and these images were removed from the dataset. Subjects of whom only two MR scans were available (one pre-operative scan and one post-operative scan) were also eliminated from the study. This is because their scans did

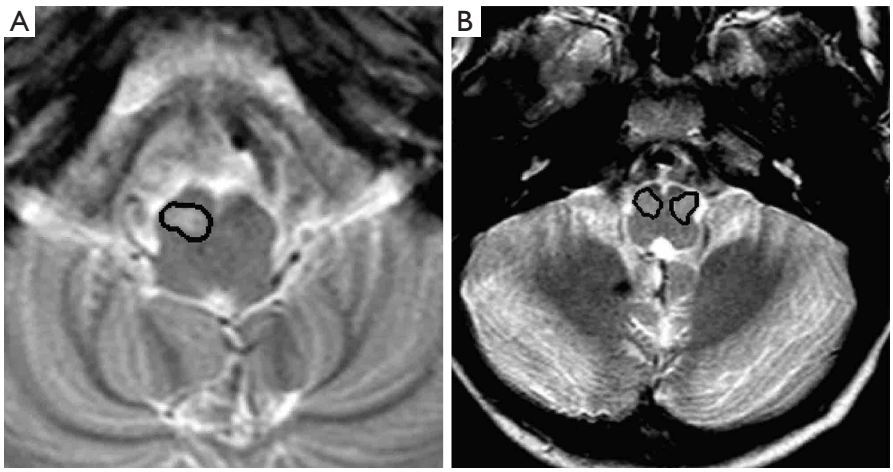

Figure 3 Axial T2 weighted images showing examples of segmentation of the inferior olivary nuclei in unilateral HOD (A) and bilateral HOD (B). Reproduced from our previous publication (18). HOD, hypertrophic olivary degeneration.

not provide enough data points over the follow-up period to allow the computation of a reliable average gradient of the size and intensity of each ION.

This resulted in a dataset of 28 subjects, all of whom had a pre-operative and at least two post-operative scans.

Image processing

The ION was initially segmented from the axial T2 weighted images. The non-volumetric acquisition of the T2 TSE sequence necessitated the segmentation to be performed on two-dimensional image slices. The segmentation was performed using a semi-automated seed growing technique with the manual placing of an arbitrary seed-point within the ION based on its anatomical landmarks. The region of interest (ROI) was obtained by growing the region from the seed, based on the grey-level signal intensity of the pixels (*Figure 3*). The segmentation was carried out thrice for each MR image to assess intra-observer variability. The initial segmentation dataset was validated by an expert neuroradiologist and was amended where necessary.

Feature extraction

Once segmented, a set of features was extracted from each ION (*Table 1*). As HOD is characterized by increase in size and T2 signal of the ION, the signal contrast between the ION and surrounding tissue (Weber contrast) and area of each ION was obtained. Including the preoperative and immediate postoperative scan, each patient had up to 6 MR scans at different time points until 1 year post surgery. In order to quantify the characteristics longitudinally during the time period, the mean gradient and variance of gradient of ION area against time were calculated for each side in

Table 1 Features used for quantitative analysis

Feature	Definition
1	Mean gradient of Weber contrast against time (left)
2	Variance of Weber contrast (left)
3	Mean gradient of the area of ION (left)
4	Variance of the area of ION (left)
5	Mean gradient of Weber contrast against time (right)
6	Variance of Weber contrast (right)
7	Mean gradient of the area of ION (right)
8	Variance of the area of ION (right)
9	Presence of HOD†
10	Bilateral HOD†
11	Unilateral HOD†
12	Hypertrophy of the olivary nucleus†
13	Gender†
14	Age at surgery†
15	Random noise (1)‡
16	Random noise (21)‡

†, features 9 to 14 were obtained from the qualitative analysis and patient demographics; ‡, features 15 and 16 represent random noise, which were added to assess the discriminative ability of the feature selection algorithms used later. Table adapted from our earlier publication (18). ION, inferior olivary nucleus; HOD, hypertrophic olivary degeneration.

Table 2 Relationship of POPCMS to the presence of HOD on qualitative analysis

POPCMS status	HOD +ve	HOD –ve	Bilateral HOD	Unilateral HOD
POPCMS present	10	5	7	3 (1 Rt/2 Lt)
POPCMS absent	5	28	2	3 (1 Rt/2 Lt)
Total	15	33	9	6

+ve, positive; –ve, negative; POPCMS, postoperative pediatric cerebellar mutism; HOD, hypertrophic olivary degeneration; Rt, right; Lt, left.

each patient. Similarly the mean and variance of gradient of contrast against time were calculated. In addition, features obtained from the radiological assessment, age and gender were also included (*Table 1*).

Feature selection and classification

Machine learning methods were used to analyse the performance of various imaging features extracted to the occurrence of POPCMS. This process involved selecting the subset of features listed in *Table 1* prior to classification of the patients into POPCMS and non-POPCMS. The techniques used were random subset feature selection (RSFS), sequential forward selection (SFS) and sequential floating forward selection (SFFS) to obtain the most relevant subsets (18,22-24). These algorithms were carried out 100 times each to obtain the average relevance scores. All the feature selection methods were performed on the three independent segmentation data sets to assess for differences due to interobserver and intraobserver variability.

Binary classification was used to assess the ability of the most relevant feature subsets to discriminate patients who developed POPCMS from those who did not. Support vector machine (SVM) was used to perform the binary classification. The entire feature set was used in addition to relevant feature subsets chosen by RSFS, SFS and SFFS algorithms.

Statistical analysis

Patients with or without POPCMS were compared with respect to the qualitative analysis data collected from the radiologist's assessment for presence or absence of HOD. The sensitivity, specificity, and accuracy measures were calculated for each variable using the standard formulas. Statistical analysis was performed using the Fisher exact test for association between HOD and POPCMS. Statistical analysis was performed using SPSS version 20.0, and P values <0.05 were considered statistically significant.

Results

Qualitative analysis

Fifteen of the 48 children included in the study were diagnosed with POPCMS.

On qualitative analysis of the MRI scans, HOD was identified in 15 children and among 9 of these 15 bilateral HOD was identified. There was significant association between POPCMS and presence of HOD (P=0.001; Relative risk =4.4; 95% confidence interval =1.8, 10.6) (*Table 2*). There was significant association between POPCMS and bilateral HOD (P=0.002; relative risk =3.8; 95% confidence interval =1.8, 7.7) and not unilateral HOD (P=0.08; RR =3.9; 95% confidence interval =1.1, 10.2) (*Table 2*). There was 100% agreement between both radiologists in identifying HOD. In seven cases there was disagreement between the radiologists with relation to hypertrophy of the ION but this did not influence the identification of HOD as there was unequivocal T2 prolongation in these cases.

Quantitative analysis

Full details of the results from the quantitative analysis is available in our earlier publication (18). The salient findings are presented in this article.

In the quantitative analysis subgroup that consisted of 28 children, 9 were diagnosed with POPCMS. Thirteen of these patients showed HOD on radiological assessment (9 bilateral and 4 unilateral). Binary classification using the entire feature set showed that Feature 1, the mean gradient of contrast in the left ION obtained the highest score for all feature selection techniques (*Table 3*) (18,19). Feature 4, the variance in the area of the left ION also showed a high score in relation to development of PPCMS (18). Features 9 and 10 that represent radiological identification of HOD and bilateral HOD respectively also showed high relevance scores in keeping with the qualitative analysis.

Analysis of the feature subsets chosen by RSFS, SFS and SFFS algorithms also indicated that feature 1 was the most

Table 3 Average relevance scores over 100 iterations using random subset feature selection algorithm

Segmentation	Features†															
Test number	1	2	3	4	5	6	7	8	9	10	11	12	13	14	15	16
1	6.22	1.61	1.08	1.81	1.64	0.23	0.65	0.11	1.06	0.94	0.16	0.03	0.42	0.09	0.00	0.00
2	8.99	0.09	0.31	1.41	1.03	0.20	0.28	1.22	0.92	1.77	0.27	0.10	1.28	0.30	0.00	0.00
3	10.03	1.24	0.00	0.42	0.00	0.12	1.62	0.15	1.19	1.46	0.00	0.00	0.18	0.59	0.00	0.00
Average	8.41	0.98	0.46	1.21	0.89	0.18	0.85	0.49	1.06	1.39	0.14	0.04	0.63	0.33	0.00	0.00

†, feature key—see *Table 1*. Table adapted from our earlier publication (18).

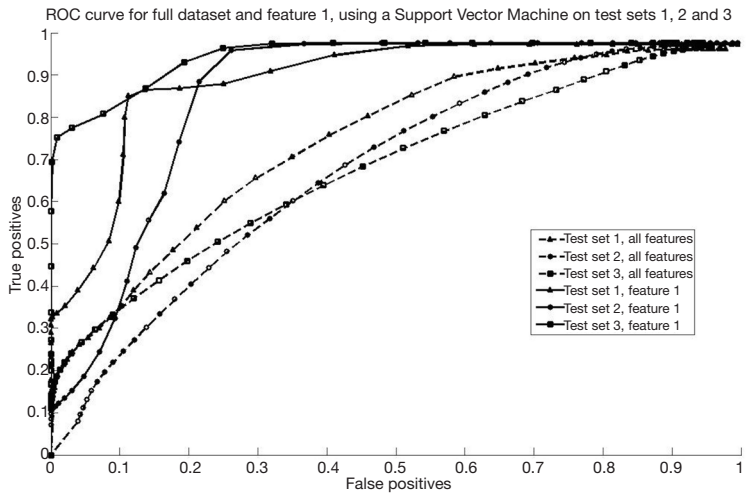

Figure 4 The receiver operating characteristic (ROC) curve for the support vector machine classifier used on the full feature dataset and feature 1 on test sets 1, 2 and 3. Reproduced from our previous publication (18).

relevant. The results obtained using the SVM classifier is shown in *Figure 4*. It is evident that an increase in classifier accuracy occurs when the least relevant features were eliminated from the feature set, keeping only the "Mean gradient of Weber contrast in the left ION". The SVM classifier produced an area under the curve (AUC) of 0.80, 0.61 and 0.70, respectively for each test set prior to feature selection (18).These values were increased to 0.93, 0.71 and 0.91, respectively when patients were classified using solely the "Mean gradient of Weber contrast in the left ION" as a feature (18). An increase in AUC indicates an increase in classifier accuracy as less relevant features are eliminated. This indicates that the "Mean gradient of Weber contrast in the left ION" is a reliable marker of POPCMS.

Discussion

Qualitative analysis of the follow up scans in our patient population has shown significant association between the occurrence of HOD and POPCMS. The temporal relationship of both conditions with posterior fossa tumour resection strengthens the view that injury to pECP is central to their causations. The strong association between bilateral HOD and POPCMS is consistent with the known association between bilateral pECP injury and POPCMS (8,10,12,15). There is very limited published literature on association between HOD and POPCMS. Patay and colleagues recently published a study comparing 12 children with and without POPCMS (25). They noticed a strong association between bilateral HOD and POPCMS ($P<0.0001$). Among the 12 patients with POPCMS, 9 had bilateral HOD and 2 had unilateral HOD. Among the 12 patients without POPCMS 10 had no evidence of HOD and only 2 had unilateral HOD. They propose that bilateral HOD is a good surrogate imaging marker for POPCMS. Allowing for minimal differences in methodology, our study has shown similar results with qualitative assessment for HOD. In both studies, equivocal changes in the ION

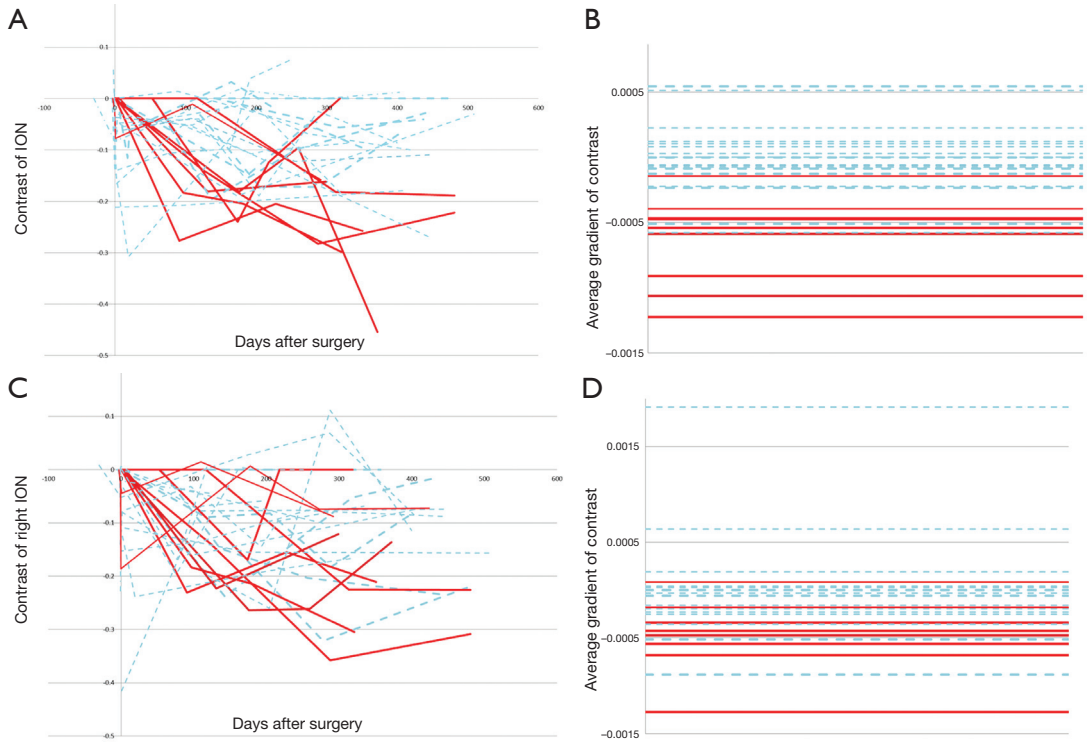

Figure 5 Graphical representation of the contrast in intensity of left ION (A) and right ION (B) and the surrounding brainstem against days after surgery. The Bold red lines represent cases with POPCMS and the dotted blue lines represent cases without POPCMS. Graph of the average gradient of contrast in the left ION (C) and right ION (D) show clear difference in average gradient between POPCMS and non-POPCMS groups in the left ION (C) compared to the right (D). ION, inferior olivary nucleus; POPCMS, postoperative pediatric cerebellar mutism.

were not regarded as positive for HOD thereby reducing subjective bias and in our study there was 100% consensus between the two radiologists in identifying HOD. This reinforces the utility of HOD as a simple imaging marker for POPCMS.

The ION is a relatively small structure in the medulla and visual assessment is limited by image resolution. As a consequence, subtle differences in signal and size of the ION will be difficult to appreciate by human assessment. The semi-automated quantitative analysis of the ION was extremely valuable in our study in accurately identifying changes in contrast between the ION and surrounding tissue and identifying subtle changes in size of the structure. The mean gradient of contrast in the left ION is the most relevant feature that correlates with POPCMS. This feature is at least five times higher than all other features and at least six times as predictive as the radiological identification of HOD or bilateral HOD (*Table 3*). This feature corresponds to the rate of change of signal contrast (i.e., contrast with the surrounding tissue) in the left ION over the follow up period, a feature that will be difficult to analyze qualitatively by the radiologist. *Figure 5* illustrates the differences in the gradients of signal intensity between the left and right ION.

HOD occurs due to trans-synaptic degeneration where the olivary deafferentiation leads to hypertrophic degeneration of the ION. With reference to the Guillain and Mollaret triangle, lesions involving the contralateral DN, SCP and ipsilateral red nucleus and central tegmental tract result in HOD whereas injury to the inferior cerebellar peduncle that carries efferent fibers from the ION is thought not to result in HOD (17). Although ipsilateral brain stem lesion can cause HOD, we believe that injury to the contralateral pECP structures (DN, SCP) can account for HOD in the setting on POPCMS. It is important to understand that HOD is a consequence of an insult that is common to that of causing POPCMS and cannot be directly implicated in the pathogenesis of mutism. HOD

has been associated with symptomatic palatal myoclonus but this clinical finding was not noticed in our patient cohort. Similar absence of palatal myoclonus was also seen in the patient cohort of Patay and colleagues who speculate that the development of palatal myoclonus may require involvement of brainstem structures adjacent to the rubro-olivary segment of the Guillain and Mollaret triangle than the pECP (25).

Unilateral HOD was not significantly associated with POPCMS in our group. Of the 6 children with unilateral HOD 3 had POPCMS (2 left sided and 1 right sided HOD) Similarly Patay and colleagues did not find a significant association between unilateral HOD and POPCMS (2 among the 4 cases with HOD had POPCMS). Our quantitative analysis has yielded an important feature of laterality with signal change in the left ION emerging as highly predictive of POPCMS. Based on the earlier discussion on HOD, this feature is likely related to right sided pECP injury. This cannot be equated to just unilateral left sided HOD but bilateral HOD as well with greater change in the left ION. Based on our result we believe that pECP injury to the right DTC pathway is an important contributor to the pathogenesis of POPCMS. To our knowledge this is the second study to date that indicates an element of laterality in the pathogenesis of POPCMS. Law and colleagues in a recently published study showed significant association between POPCMS and compromise of right cerebellar white matter in the cerebello-thalamo-cerebellar pathway ($P<0.02$) based on diffusion tensor imaging (6). They speculate that disruption of the right cerebellar white matter deprives the left cerebral language areas from modulatory signals required for language processing (26). The left hemisphere dominance for language function in majority of the population also justifies this hypothesis (27,28). This has an important implication and could influence surgical approach and risk assessment in tumours that closely related to the right pECP.

The temporal evolution of HOD has been divided into six stages based on pathology assessment (29) but its evolution has been divided into three stages based on MRI (17). The first stage can be noted as early as 4 weeks following insult with increased signal intensity of the ION on T2 weighted and proton density images. The second stage involves hypertrophy and T2 hyperintensity of the ION appearing usually 6 months after the insult and lasting 3–4 years. The final stage begins with resolution of hypertrophy with persisting hyperintensity and lasts indefinitely. The rationale to limit the follow up period to 1 year was that the first two stages of HOD can be captured during this period and it is unlikely for children to develop HOD after a year post surgery. As the MR images were performed at different time points and frequency for each patient, we chose to perform a longitudinal analysis, which was more reliable than a cross-sectional study at a specific time point. In order to assess for HOD, it is required to quantify the change in intensity and size of the ION over time necessitating a comparison between at least two episodes MRI for each patient. We analysed patients with 3 or more follow-up scan including the immediate postoperative scan in order to obtain enough data points to allow a reliable average gradient of change in intensity and area to be calculated. Such features give insight to how the ION is changing over time.

Patay and colleagues noticed 100% specificity of bilateral HOD. In our group, 2 children with bilateral HOD did not have POPCMS (*Table 2*). The reason for this is unclear but may be related to the involvement of specific structures of the Guillain and Mollaret triangle that may not be associated with POPCMS. Five of our patients with POPCMS did not show any evidence of HOD (*Table 2*) on qualitative analysis and from the results of the quantitative analysis we believe that this could be partly explained by the limitations of visual examination in identifying subtle changes to the ION. In our methodology, cases with equivocal findings were not considered positive for HOD.

One of the limitations of the study was that an identical cohort could not be obtained for the qualitative and quantitative analysis. Secondly, volumetric imaging of the ION would have increased the accuracy of the results. These are mainly attributed to the retrospective nature of the study. These limitations are however offset by the highly convincing results related to the left ION. We hope to validate this in the future in a larger cohort. An important issue related to POPCMS in the past has been the wide variations in the definition of this condition. We believe that our definition is close to that proposed to the recently published definition based on the recently published consensus paper on POPCMS (1).

Conclusions

This study provides qualitative and quantitative evidence of the strong association between HOD and POPCMS. The outcome of our study has important clinical and research implications on POPCMS. Bilateral HOD following posterior fossa tumour resection can be a

reliable radiological indicator of POPCMS and may help establishing the diagnosis of POPCMS in children with equivocal clinical findings. This is the first study to evaluate HOD using semi automated image analysis in addition to qualitative analysis and has demonstrated the significance of left ION changes that are indicative of right pECP injury. We believe that this is an important factor in pathogenesis of POPCMS. The laterality of the tumour and its relationship to the pECP could influence surgical strategy in the future and will need validation in a larger patient cohort.

Acknowledgements

None.

Footnote

Conflicts of Interest: The authors have no conflicts of interest to declare.

Ethical Statement: The study methodology was granted approval by the Institutional Research Director.

References

1. Gudrunardottir T, Morgan AT, Lux AL, Walker DA, Walsh KS, Wells EM, Wisoff JH, Juhler M, Schmahmann JD, Keating RF, Catsman-Berrevoets C14; Iceland Delphi Group. Consensus paper on post-operative pediatric cerebellar mutism syndrome: the Iceland Delphi results. Childs Nerv Syst 2016;32:1195-203.
2. De Smet HJ, Baillieux H, Catsman-Berrevoets C, De Deyn PP, Mariën P, Paquier PF. Postoperative motor speech production in children with the syndrome of 'cerebellar' mutism and subsequent dysarthria: a critical review of the literature. Eur J Paediatr Neurol 2007;11:193-207.
3. Huber JF, Bradley K, Spiegler BJ, Dennis M. Long-term effects of transient cerebellar mutism after cerebellar astrocytoma or medulloblastoma tumor resection in childhood. Childs Nerv Syst 2006;22:132-8.
4. Steinbok P, Cochrane DD, Perrin R, Price A. Mutism after posterior fossa tumour resection in children: incomplete recovery on long-term follow-up. Pediatr Neurosurg 2003;39:179-83.
5. Aguiar PH, Plese JP, Ciquini O, Marino R. Transient mutism following a posterior fossa approach to cerebellar tumors in children: a critical review of the literature. Childs Nerv Syst 1995;11:306-10.
6. Law N, Greenberg M, Bouffet E, Taylor MD, Laughlin S, Strother D, Fryer C, McConnell D, Hukin J, Kaise C, Wang F, Mabbott DJ. Clinical and neuroanatomical predictors of cerebellar mutism syndrome. Neuro Oncol 2012;14:1294-303.
7. Sagiuchi T, Ishii K, Aoki Y, Kan S, Utsuki S, Tanaka R, Fujii K, Hayakawa K. Bilateral crossed cerebello-cerebral diaschisis and mutism after surgery for cerebellar medulloblastoma. Ann Nucl Med 2001;15:157-60.
8. Avula S, Kumar R, Pizer B, Pettorini B, Abernethy L, Garlick D, Mallucci C. Diffusion abnormalities on intraoperative magnetic resonance imaging as an early predictor for the risk of posterior fossa syndrome. Neuro Oncol 2015;17:614-22.
9. Miller NG, Reddick WE, Kocak M, Glass JO, Löbel U, Morris B, Gajjar A, Patay Z. Cerebellocerebral diaschisis is the likely mechanism of postsurgical posterior fossa syndrome in pediatric patients with midline cerebellar tumors. AJNR Am J Neuroradiol 2010;31:288-94.
10. Morris EB, Phillips NS, Laningham FH, Patay Z, Gajjar A, Wallace D, Boop F, Sanford R, Ness KK, Ogg RJ. Proximal dentatothalamocortical tract involvement in posterior fossa syndrome. Brain 2009;132:3087-95.
11. Ojemann JG, Partridge SC, Poliakov AV, Niazi TN, Shaw DW, Ishak GE, Lee A, Browd SR, Geyer JR, Ellenbogen RG. Diffusion tensor imaging of the superior cerebellar peduncle identifies patients with posterior fossa syndrome. Childs Nerv Syst 2013;29:2071-7.
12. Puget S, Boddaert N, Viguier D, Kieffer V, Bulteau C, Garnett M, Callu D, Sainte-Rose C, Kalifa C, Dellatolas G, Grill J. Injuries to inferior vermis and dentate nuclei predict poor neurological and neuropsychological outcome in children with malignant posterior fossa tumors. Cancer 2009;115:1338-47.
13. van Dongen HR, Catsman-Berrevoets CE, van Mourik M. The syndrome of 'cerebellar' mutism and subsequent dysarthria. Neurology 1994;44:2040-6.
14. Wells EM, Khademian ZP, Walsh KS, Vezina G, Sposto R, Keating RF, Packer RJ. Postoperative cerebellar mutism syndrome following treatment of medulloblastoma: neuroradiographic features and origin. J Neurosurg Pediatr 2010;5:329-34.
15. Crutchfield JS, Sawaya R, Meyers CA, Moore BD 3rd. Postoperative mutism in neurosurgery. Report of two cases. J Neurosurg 1994;81:115-21.
16. Avula S, Mallucci C, Kumar R, Pizer B. Posterior fossa syndrome following brain tumour resection: review of

pathophysiology and a new hypothesis on its pathogenesis. Childs Nerv Syst 2015;31:1859-67.
17. Goyal M, Versnick E, Tuite P, Cyr JS, Kucharczyk W, Montanera W, Willinsky R, Mikulis D. Hypertrophic olivary degeneration: metaanalysis of the temporal evolution of MR findings. AJNR Am J Neuroradiol 2000;21:1073-7.
18. Spiteri M, Windridge D, Avula S, Kumar R, Lewis E. Identifying quantitative imaging features of posterior fossa syndrome in longitudinal MRI. J Med Imaging (Bellingham) 2015;2:044502.
19. Abernethy LJ, Avula S, Hughes GM, Wright EJ, Mallucci CL. Intra-operative 3-T MRI for paediatric brain tumours: challenges and perspectives. Pediatr Radiol 2012;42:147-57.
20. Avula S, Mallucci CL, Pizer B, Garlick D, Crooks D, Abernethy LJ. Intraoperative 3-Tesla MRI in the management of paediatric cranial tumours--initial experience. Pediatr Radiol 2012;42:158-67.
21. Dailey AT, McKhann GM 2nd, Berger MS. The pathophysiology of oral pharyngeal apraxia and mutism following posterior fossa tumor resection in children. J Neurosurg 1995;83:467-75.
22. Pohjalainen J, Räsänen O, Kadioglu S. Feature selection methods and their combinations in high-dimensional classification of speaker likability, intelligibility and personality traits. Computer Speech & Language 2015;29:145-71.
23. Whitney AW. A direct method of nonparametric measurement selection. IEEE Transactions on Computers 1971;20:1100-3.
24. Räsänen O, Pohjalainen J. Random subset feature selection in automatic recognition of developmental disorders, affective states, and level of conflict from speech. Lyon: Proc Interspeech, 2013.
25. Patay Z, Enterkin J, Harreld JH, Yuan Y, Löbel U, Rumboldt Z, Khan R, Boop F. MR imaging evaluation of inferior olivary nuclei: comparison of postoperative subjects with and without posterior fossa syndrome. AJNR Am J Neuroradiol 2014;35:797-802.
26. Fiez JA, Petersen SE, Cheney MK, Raichle ME. Impaired non-motor learning and error detection associated with cerebellar damage. A single case study. Brain 1992;115 Pt 1:155-78.
27. Knecht S, Deppe M, Dräger B, Bobe L, Lohmann H, Ringelstein E, Henningsen H. Language lateralization in healthy right-handers. Brain 2000;123:74-81.
28. Knecht S, Dräger B, Deppe M, Bobe L, Lohmann H, Flöel A, Ringelstein EB, Henningsen H. Handedness and hemispheric language dominance in healthy humans. Brain 2000;123 Pt 12:2512-8.
29. Goto N, Kaneko M. Olivary enlargement: chronological and morphometric analyses. Acta Neuropathol 1981;54:275-82.

Cite this article as: Avula S, Spiteri M, Kumar R, Lewis E, Harave S, Windridge D, Ong C, Pizer B. Post-operative pediatric cerebellar mutism syndrome and its association with hypertrophic olivary degeneration. Quant Imaging Med Surg 2016;6(5):535-544. doi: 10.21037/qims.2016.10.11

